Neural agrin controls acetylcholine receptor stability in skeletal muscle fibers

Gabriela Bezakova*†, Inger Rabben*, Iren Sefland*, Guido Fumagalli‡, and Terje Lømo*§

*Department of Physiology, University of Oslo, 0317 Oslo, Norway; and ‡Department of Medicine and Public Health, University of Verona, Ospedale Borgo Roma, 37134 Verona, Italy

Edited by Bert Sakmann, Max Planck Institute for Medical Research, Heidelberg, Germany, and approved June 19, 2001 (received for review November 13, 2000)

At mammalian neuromuscular junctions (NMJs), innervation induces and maintains the metabolic stability of acetylcholine receptors (AChRs). To explore whether neural agrin may cause similar receptor stabilization, we injected neural agrin cDNA of increasing transfection efficiencies into denervated adult rat soleus (SOL) muscles. As the efficiency increased, the amount of recombinant neural agrin expressed in the muscles also increased. This agrin aggregated AChRs on muscle fibers, whose half-life increased in a dose-dependent way from 1 to 10 days. Electrical muscle stimulation enhanced the stability of AChRs with short half-lives. Therefore, neural agrin can stabilize aggregated AChRs in a concentration- and activity-dependent way. However, there was no effect of stimulation on AChRs with a long half-life (10 days). Thus, at sufficiently high concentrations, neural agrin alone can stabilize AChRs to levels characteristic of innervated NMJs.

The postsynaptic membrane of normal neuromuscular junctions (NMJs) contains acetylcholine receptors (AChRs) that have a high metabolic stability ($t_{1/2}$ = ≈10 days). This stability is induced and maintained by innervation. In development, motor axons contact skeletal muscle fibers, aggregate AChRs in underlying muscle membrane, and increase the half-life of aggregated AChRs from about 1 to 10 days (1, 2). Following denervation, the postsynaptic AChRs lose this stability. The AChRs present in the postsynaptic membrane at the time of denervation acquire a half-life of 3–7 days ("old" AChRs) and are replaced by "new" AChRs. In the mouse, the half-life of the new junctional AChRs is the same as that of extrajunctional AChRs in denervated fibers (≈1 day; ref. 3), whereas in the rat it is longer (2.1–3.6 days; refs. 4–6). Reinnervation restores a half-life of 10 days to the old AChRs, blocks the expression of new unstable AChRs, and induces the appearance of new stable AChRs (7, 8). Like reinnervation, electrical stimulation of denervated muscles blocks the expression of unstable AChRs and induces the appearance of stable AChRs (4, 6). Unlike reinnervation, however, electrical stimulation fails to restabilize the old AChRs in the postsynaptic membrane, suggesting that a nerve-derived trophic factor is required (5).

Here we examine whether neural agrin is one such nerve-derived factor. Neural agrin, which is released by motor nerve terminals into the synaptic cleft (9), is essential for the formation of NMJs (10). Furthermore, when released from muscle fibers transfected by neural agrin cDNA, recombinant agrin induces a postsynaptic-like apparatus on muscle fibers (11, 12). We have therefore injected neural agrin cDNA of different transfection efficiencies into rat soleus (SOL) muscles and measured amount of neural agrin and metabolic stability of aggregated AChRs for each efficiency. The results show that the half-lives range from 1 to 10 days depending on the amount of neural agrin in the muscle.

Materials and Methods

Surgical Procedures and *in Vivo* Stimulation. The experiments were carried out on adult male Wistar rats (body weight ≈250 g). All surgical procedures were done under deep anesthesia by Equithesin (0.4 ml/100 g, i.p.) in the absence of skin or muscle reflexes. SOL was denervated by removing ≈5 mm of the sciatic nerve in the thigh. Fifty microliters of purified neural agrin cDNA in PBS was then injected into the proximal third of the exposed SOL with a fine needle. Eight days later, 50 μl of 1.0 μM rhodamine-conjugated α-bungarotoxin (Rh-BuTx) was injected into the SOL. This dose appeared to saturate the AChRs because no further labeling occurred when fluorescein-conjugated α-bungarotoxin (Fl-BuTx) was injected 2 h after Rh-BuTx. For stimulation, uninsulated ends of two wires (AS 632, Cooner, Chatsworth, CA) were, in addition, placed across the SOL (see ref. 13 for details). Stimulation started 1 h later and consisted of 60 0.4-ms-long bipolar square pulses at 100 Hz every 60 s for up to 9 days. The experiments were conducted in conformity with the laws and regulations for experiments on live animals in Norway and overseen by the veterinarian responsible for the animal house.

DNA Preparation. Full-length rat agrin-Y4Z8 cDNA in pcDNA with a CMV promoter (14) was purified by using either the Jet Star plasmid DNA purification kit (Genomed, Bad Oeynhausen, Germany) or the plasmid maxiprep system Concert (GIBCO). The purified plasmid was then diluted in PBS (pH 7.4). Unexpectedly, the second purification procedure resulted in considerably higher transfection efficiency than the first for the same amount of injected DNA. We used this finding to obtain DNA solutions of three different transfection efficiencies, resulting in relatively low, intermediate, and high amounts of neural agrin in transfected muscles (Fig. 1*a*). Later, we refer to these conditions as nAgrin-low (0.2 μg/μl, first purification procedure), nAgrin-medium (2.0 μg/μl, first purification procedure), and nAgrin-high (2.0 μg/μl, second purification procedure), respectively. In some experiments, 0.2 μg/μl DNA purified by the second procedure was also used.

GFP-Tagged Agrin Expression Construct. Full-length rat agrin-Y4Z8 was digested with restriction enzymes *Sal*I and *Eco*RV and made blunt. This digestion removed the sequence encoding amino acids 344 to 1415. The pEGFP-C1 vector (CLONTECH) was digested with *Nhe*I and *Xho*I and blunted. The 752-bp fragment containing the entire coding sequence for EGFP without stop codon was fused in frame into neural agrin Y4Z8 between sites encoding amino acids 343 and 1416 in the pcDNA vector. The resulting GFP-tagged construct was purified as described above

This paper was submitted directly (Track II) to the PNAS office.

Abbreviations: AChR, acetylcholine receptor; NMJ, neuromuscular junction; SOL, soleus muscle; Rh-BuTx, rhodamine conjugated α-bungarotoxin; Fl-BuTx, fluorescein-conjugated α-bungarotoxin.

†Present address: Department of Pharmacology, Biozentrum, University of Basel, 4056 Basel, Switzerland.

§To whom reprint requests should be addressed at: Department of Physiology, P.O. Box 1103, Blindern, 0317 Oslo, Norway. E-mail: terje.lomo@basalmed.uio.no.

The publication costs of this article were defrayed in part by page charge payment. This article must therefore be hereby marked "*advertisement*" in accordance with 18 U.S.C. §1734 solely to indicate this fact.

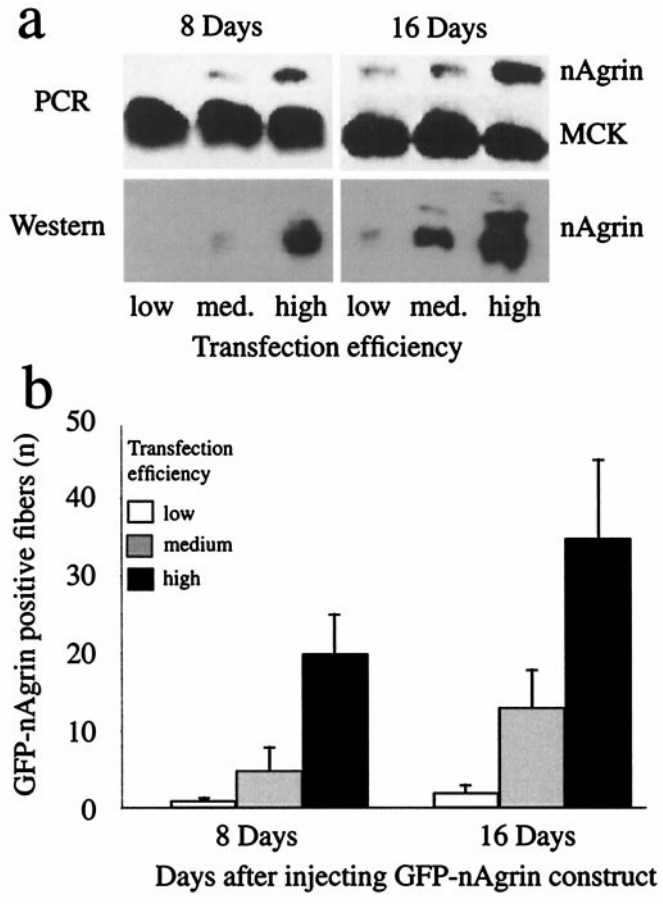

Fig. 1. Neural agrin mRNA, recombinant protein, and positive fibers in SOL muscles injected with neural agrin cDNA. SOL muscles were examined 8 and 16 days after injections of full-length (*a*) or GFP-tagged (*b*) rat neural agrin cDNA of low, medium, or high transfection efficiency, as indicated. Note the increase in the amount of recombinant neural agrin mRNA (by PCR) and protein (by Western blots) in *a* and the number of GFP-positive fibers in *b* (±SD, fibers from two muscles) for each increase in transfection efficiency. Amount of mRNA for muscle creatine kinase (MCK), a ''housekeeping'' gene, was essentially unaffected. Results in *a* are representative of results from three (PCR) and two (Western) muscles.

and used at 0.2 μg/μl and 2.0 μg/μl. The number of GFP-positive fibers was counted in small fiber bundles teased from whole muscles and summed.

Analysis of Agrin mRNA By Using PCR Amplification. SOL muscles were removed 8 and 16 days after DNA injection, immediately frozen in liquid nitrogen, and extracted for RNA by using acidic phenol. The mRNA was reverse-transcribed with Superscript reverse transcriptase (GIBCO), using random hexamer primers. PCR at 56°C was performed, using primers CCGTAAGGGATGACTGTGAA and TTGAGTTGCGAGACTGGTT for agrin and TGAGCAAGCACCCCAAGTTT and GATCATGTCGTCGATGGACT for muscle creatine kinase (MCK). Amplified nAgrin and MCK products were resolved on 1% agarose gel and shown to have sizes of 600 bp and ≈230 bp, respectively.

Immunoprecipitation and Western Blot. SOL muscles were removed, frozen in liquid nitrogen, and homogenized at pH 7.4 in 10 vol (wt/vol) of ice-cold homogenization buffer (HB) containing 10 mM sodium phosphate, 150 mM NaCl, 5 mM EDTA, 2 mM PMSF, and protease inhibitors aprotinin, leupeptin, benzamidin, and pepstatin (0.5 μg/ml each), using a Polytron. After centrifugation (20 min at 50,000 × *g*), the supernatant was incubated with monoclonal antibody against rat agrin A86 (StressGen Biotechnologies, Victoria, Canada) overnight at 4°C. Protein G Sepharose (Sigma) was added for 4 h at 4°C. The beads were then applied on a column and washed with 50 vol of HB. Bound agrin was eluted with 50 μl of sample buffer and loaded on 3–12% SDS/PAGE gel. Proteins were transferred to nitrocellulose membrane by using standard methods (15). After blocking, the membranes were incubated overnight with monoclonal antibody against rat agrin A86 and then with goat anti mouse antibody conjugated to HRP (Jackson ImmunoResearch) diluted 1:2,000. Bands were visualized by chemiluminescence (Pierce) and exposed to film (Kodak).

Determination of AChR Half Lives. At different times after injection of Rh-BuTx, SOL muscles were removed, fixed with 1.5% paraformaldehyde, dissected into small bundles (≈30 per muscle), stained with FITC-BuTx (Sigma), and examined with an AX70 fluorescence microscope (Olympus, New Hyde Park, NY). Images were captured with a Color Coolview CCD camera (Photonic Science, East Sussex, U.K.) and OPENLAB imaging software (Improvision, Coventry, U.K.). Rhodamine-labeled images of NMJs or agrin-induced AChR aggregates seen on the surface of the bundles were quantified. The imaging system was calibrated, using the InSpeck Microscope Image Intensity Calibration Kit (Molecular Probes) containing microspheres coated with six different concentrations of fluorescent dye (see ref. 16). Collections of closely adjacent AChR aggregates that stood out as separate, were larger than 20 μm^2, and could be viewed in their entirety on the surface of individual muscle fibers were selected for measurements. Specific intensity was calculated as the mean pixel intensity of each collection minus the mean pixel intensity of an adjacent and AChR aggregate-free portion of the fiber. This value was then normalized to the value given by microspheres coated with 3% of fluorescent dye in the same session. The slope of the line, which best fit the experimental values at each time point (mean ± SEM), provided the half-life.

Immunocytochemistry. A mouse monoclonal antibody (Agrin-86) against neural agrin (Y4Z8, StressGen) and rabbit polyclonal antibodies against AChR ε- or γ-subunits were used (17). Muscles were fixed in 1.5% paraformaldehyde. For labeling of agrin and ε-subunits, bundles were permeabilized by using 1% Triton X-100. For labeling of γ-subunits, the muscle bundles were permeabilized with ice-cold methanol at −20°C for 15 min, incubated for 3–5 min with 50 mM ethylamine (pH 11.0) at room temperature, and rinsed for 30 min in PBS with 1% BSA (18). Bundles were incubated overnight at 4°C with primary antibodies diluted 1:200 in PBS and 1% BSA. FITC-conjugated anti-mouse or anti-rabbit secondary antibodies (Sigma) were used at dilution 1:200. The samples were observed with confocal scanning laser microscope TCS-SP (Leica Microsystems, Heidelberg, Germany).

Results

Expression of Increasing Amounts of Recombinant Neural Agrin. To vary the amount of neural agrin in SOL muscles, we injected solutions of neural agrin cDNA of increasing transfection efficiencies into the muscles. Using full length neural agrin cDNA (14), we quantitated transcription of mRNA and expression of recombinant protein (Fig. 1*a*). Eight days after injection of DNA solutions of low, medium, and high transfection efficiencies, the relative amounts of neural agrin mRNA amplified by PCR and normalized to ''housekeeping'' gene MCK were 0 (undetectable), 0.043 ± 0.013, and 0.155 ± 0.037, respectively. After 16 days, these values had increased to 0.09 ± 0.022, 0.143 ± 0.035, and 0.446 ± 0.093 (mean values ± SD, $n = 3$). The corresponding total amounts of immunoprecipitated agrin in percent of the

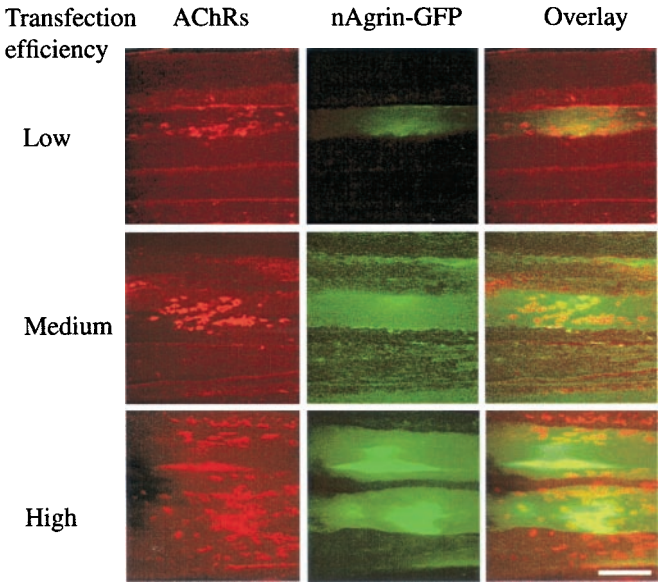

Fig. 2. Recombinant neural agrin and accompanying AChR aggregates in transfected SOL muscles. SOL muscles were denervated and injected with solutions of GFP-tagged neural agrin cDNA of low, medium, or high transfection efficiencies, as indicated. Eight days later, the muscles were removed, teased into bundles, incubated with Rh-BuTx, and examined with confocal microscope. Note the increase in the amount of recombinant GFP-tagged neural agrin (green fluorescence) and the number of AChR aggregates (red) on transfected (see overlay) and adjacent muscle fibers for each increase in transfection efficiency. (Scale bar, 50 μm.)

highest amount expressed by any of the treatments were 0 (undetectable), 6.7, and 47.3 after 8 days and 4.9, 33.7, and 100 after 16 days (mean values, $n = 2$). Below, these amounts are referred to as nAgrin-low, nAgrin-medium, and nAgrin-high. These results also indicate that agrin is continuously synthesized during the course of the experiment.

In some experiments, we used GFP-tagged neural agrin DNA. Although not full length (see *Materials and Methods*), this construct contained the C-terminal part of neural agrin and aggregated AChRs as effectively as the full-length neural agrin, as determined by visual inspection. The results confirmed, in independent experiments, that transfection efficiency could be graded by the same purification and concentration procedures as used for full-length neural agrin. The number of GFP-positive fibers (Fig. 1*b*), intensity of GFP labeling, and number of AChR aggregates (Fig. 2) increased with each increase in transfection efficiency. Fig. 2 also illustrates the appearance of the preparations and the close association between GFP-positive fibers and AChR aggregates on transfected and nontransfected neighboring fibers.

Neural Agrin Stabilizes AChRs. We then examined the effects of different amounts of recombinant neural agrin in transfected muscles on AChR stability. On day 0, we denervated the SOL and injected different solutions of full-length neural agrin cDNA. On day 8, we injected saturating concentrations of Rh-BuTx (see *Materials and Methods*) to label AChR aggregates induced by recombinant neural agrin. Labeling intensity was higher in muscles expressing nAgrin-high than nAgrin-low (see *Materials and Methods*), but not as high as at NMJs in the same muscle (Table 1), perhaps because of differences in the degree of membrane infoldings at young agrin-induced and mature nerve-induced AChR aggregates.

The labeling intensity was first measured on day 8 (Fig. 3 *a* and *a′*), 1 h after injection of Rh-BuTx. Labeling had almost disappeared on day 10 (2 days after labeling) at aggregates induced by nAgrin-low (Fig. 3*b*) but was still relatively intense on day 17 at aggregates induced by nAgrin-high (Fig. 3*b′*).

Table 1. AChR half-life and labeling intensity by Rh-BuTx at ectopic neural agrin-induced AChR aggregates and at normal NMJs

DNA efficiency	Stimulation	Pixel intensity at day 0	Half-life, days	*n*
Low	No	0.23 ± 0.07	0.86	28–64
Low	Yes		3.75*	14–64
Medium	No	0.27 ± 0.01	3.68	18–65
Medium	Yes		5.39*	17–65
High	No	0.47 ± 0.05	10.25	15–38
High	Yes		9.90	13–34
Original endplates		1.93 ± 0.08	11.10	30

SOL muscles were denervated and injected with neural agrin cDNA of different transfection efficiencies. Eight days later (day 0), Rh-BuTx was injected and mean pixel intensity at agrin-induced AChR aggregates was measured that day. Electrodes were implanted on day 0 and mean pixel intensity measured on subsequent days to determine the AChR half-life in stimulated and unstimulated muscles. Pixel intensity ± SEM; *n*, number of AChR aggregates examined.

*Significant difference ($P < 0.05$) between values in unstimulated and stimulated muscles.

To facilitate identification of aggregates that had nearly lost their Rh-BuTx label, muscles were routinely treated with Fl-BuTx at the end of the experiment to label AChRs inserted in the aggregates after injection of Rh-BuTx (Fig. 3 *c* and *c′*). Aggregates positive for Rh-BuTx were always positive for Fl-BuTx and the two stainings overlapped (compare Fig. 3 *b* and *c* and *b′* and *c′*). Given this overlap, we measured weak Rh labeling as the average intensity over a region defined by Fl-BuTx labeling. In addition, the overlap of Rh- and Fl-BuTx labeling indicated that the sites of AChR aggregation were stable over time, as previously observed for synaptic and nonsynaptic AChR clusters in culture (19).

The time-dependent reduction of mean labeling intensity at neural agrin-induced AChR aggregates was quantified from images such as those illustrated in Fig. 3. Labeling intensity declined approximately mono-exponentially with half-lives of 0.9, 3.7, and 10.3 days at aggregates induced by nAgrin-low, nAgrin-medium, and nAgrin-high, respectively (Fig. 4, Table 1). In some experiments, we also injected a 10-fold diluted solution of cDNA purified by the second procedure (see *Materials and Methods*) and found an intermediate half-life of 7.2 days (data not shown). All collections of closely adjacent AChR aggregates fulfilling the criteria of being separate and visible in their entirety on the surface of individual muscle fibers were measured.

In muscles expressing nAgrin-high, AChR aggregates may have been induced by both high and low concentrations of recombinant agrin, depending on their distance from transfected fibers. If so, greater variability and more complex degradation curves than seen in Fig. 4 might have been expected. However, binding to alpha-dystroglycan or immobilization in the membrane could have restricted diffusion of agrin. Aggregates induced by low concentrations of agrin should also have essentially disappeared by day 3 after Rh-BuTx labeling when aggregates in muscles expressing nAgrin-high were first analyzed (see Fig. 4). Regardless of the validity of these possibilities, the results clearly indicate that neural agrin alone can stabilize AChRs to levels characteristic of normal NMJs.

We examined AChR turnover at NMJs in the same muscles to confirm our method based on fluorescent BuTx and allow comparison of AChR turnover at ectopic AChR aggregates and NMJs. Junctional AChRs were labeled with a single intramus-

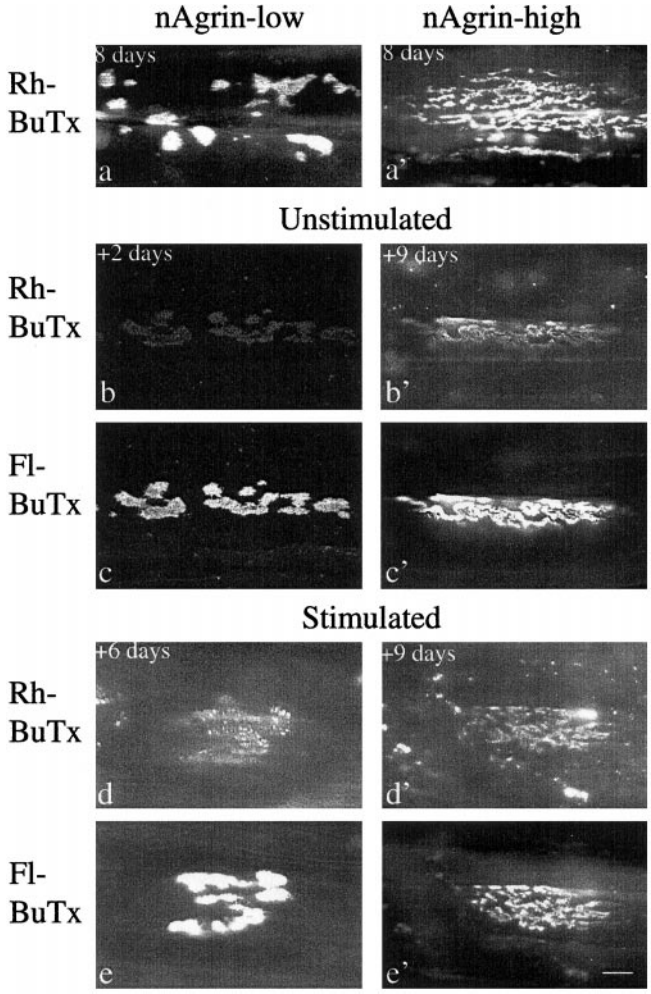

Fig. 3. AChRs at neural agrin-induced aggregates turn over at different rates. SOL muscles were denervated and injected with solutions of neural agrin (nAgrin) cDNA that resulted in expression of low or high amounts of recombinant nAgrin as indicated. Eight days later Rh-BuTx was injected into all muscles and electrical stimulation started for some of the muscles. At different times thereafter (+2 to +9 days), the muscles were removed, fixed, and labeled with Fl-BuTx to visualize AChRs inserted after day 8. In muscles expressing low amounts of nAgrin, AChR aggregates were induced whose Rh-BuTx labeling essentially disappeared in 2 days in unstimulated muscles (*b*) but was still present after 6 days in stimulated muscles (*d*). In muscles expressing high amounts of nAgrin, AChR aggregates displayed Rh-BuTx labeling as late as 9 days after Rh-BuTx injection in both unstimulated (*b′*) and stimulated (*d′*) muscle. Shown in *a* and *a′* are nAgrin-induced AChR aggregates examined 1 h after injection of Rh-BuTx. Note also that labeling by Rh- and Fl-BuTx overlap where Rh-BuTx is still present. (Scale bar, 10 μm.)

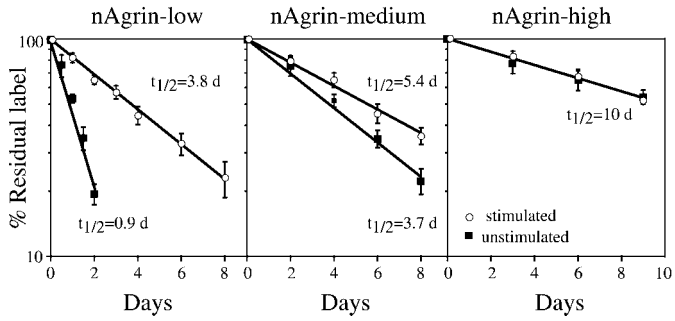

Fig. 4. Neural agrin and electrical muscle stimulation affect AChR stability. SOL muscles were injected with Rh-BuTx 8 days after denervation and injection of solutions of nAgrin cDNA that resulted in low, medium, and high amounts of recombinant nAgrin in the muscles as indicated. Relative fluorescence at nAgrin-induced AChR aggregates (ordinate, see *Materials and Methods*) declined at fast, intermediate, and slow rates in muscles expressing low, medium, or high amounts of recombinant protein (■). Electrical muscle stimulation starting on the day of Rh-BuTx injection decreased the degradation rate at AChR aggregates induced in muscles expressing low or medium but not high amounts of recombinant nAgrin (○). For each time point, 13–64 measurements were done in at least three different animals.

cular injection of Rh-BuTx. At innervated NMJs, the mean pixel intensity decayed with a half-life of 11.1 days (Table 1). At NMJs denervated immediately after the injection, the decay was first slow and then accelerated to a half-life of 4.9 days (data not shown). At NMJs denervated 8 days before the injection, the decay was biphasic, indicating the presence of two types of AChRs, one disappearing with a half-life of 2.2 days, the other with half-life of 5.3 days (data not shown). These half-lives are essentially the same as those reported earlier at rat SOL NMJs *in vivo* using radioactive ^{125}I-BuTx (4, 5).

A saturating dose of Rh-BuTx has recently been shown to cause transient destabilization of AChRs at innervated NMJs (20). We did not look for such transient destabilization at NMJs, which would have required multiple measurements from the same NMJ at earlier time points than used here. Our procedure conforms to numerous earlier studies (7) and gives comparable results. At noninnervated neural agrin-induced AChR aggregates, destabilization by BuTx is unlikely because such destabilization does not occur at NMJs denervated or inactivated by tetrodotoxin (20).

To examine the effect of neural agrin on AChR subunit composition in relation to AChR stability, we labeled ectopic AChR aggregates with antibodies specific for AChR γ- and ε-subunits. Labeling intensity for ε-subunits increased for each increase in amount of neural agrin (Fig. 5), indicating dose-dependent induction of ε-subunit expression by neural agrin. In addition, these results suggest that muscle stimulation can at least partially stabilize γ-subunit-containing AChRs, because the aggregates induced by nAgrin-low and labeled on day 8 when the stimulation started contained only or mainly γ-subunits. During stimulation, the half-life of these AChRs increased from 0.9 to 3.8 days (Fig. 4, Table 1).

Electrical Muscle Stimulation Modulates AChR Stability. To examine the effect of electrical muscle activity on AChR stability at agrin-induced aggregates, we started stimulation on day 8 soon after the injection of Rh-BuTx. Regardless of the amount of recombinant neural agrin in the muscle, the stimulation caused most of the agrin-induced aggregates to disappear (the losers) while a few aggregates survived (the winners), as described (21). Representative images of winners in Fig. 3 illustrate that stimulation causes an apparent increase in AChR stability at aggregates induced by nAgrin-low (compare Fig. 3 *b* and *d*) but has no obvious effect at aggregates induced by nAgrin-high (compare Fig. 3 *b′* and *d′*). From images such as these, we found that stimulation caused an apparent increase in AChR half-life from 0.9 to 3.8 days and 3.7 to 5.4 days in muscles expressing low and medium amounts of nAgrin, respectively (Fig. 4, Table 1). In contrast, stimulation had no effect on AChR half-life in muscles expressing high amounts of nAgrin, which remained at ≈10 days (Fig. 4, Table 1). We never found AChR aggregates in unstimulated muscles that were brightly stained by Rh-BuTx 2 days after labeling and, consequently, turned over slowly. Therefore, the partial stabilization at low and medium amounts of nAgrin must be attributed the stimulation.

Discussion

Neural agrin induces specializations in skeletal muscle fibers *in vivo* that resemble the postsynaptic specializations at NMJs (11,

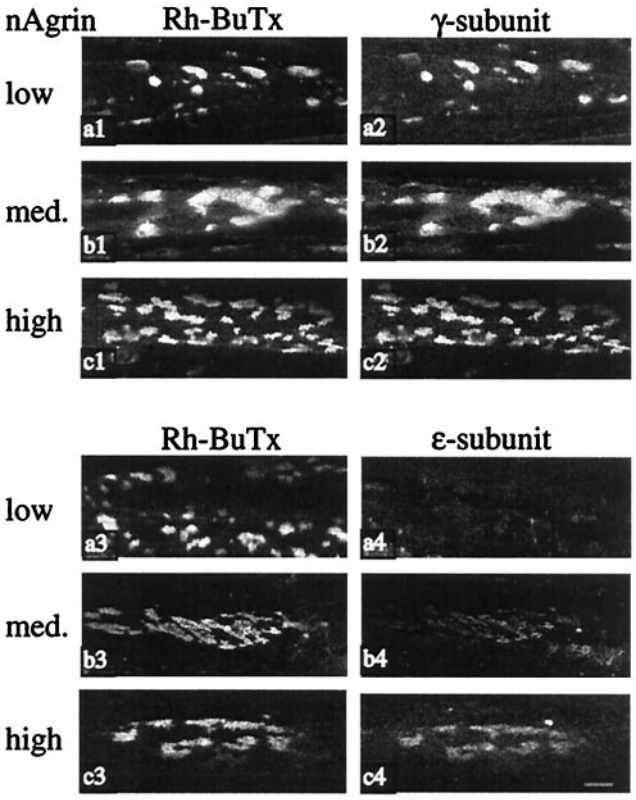

Fig. 5. γ and ε AChR subunits at nAgrin-induced AChR aggregates. SOL muscles were denervated and injected with solutions of nAgrin cDNA that resulted in the expression of low, intermediate, and high amounts of recombinant nAgrin as indicated. Eight days later, Rh-BuTx was injected into the muscles and the muscles removed 1 h later. The muscles were then incubated with antibodies against γ- or ε-subunits. Note the increase in ε-subunit labeling at AChR aggregates for each increase in the amount of recombinant neural agrin in the muscles (*a4*, *b4*, and *c4*). (Scale bar, 10 μm.)

12). We now show that neural agrin can also stabilize AChRs at such specializations in a dose-dependent way. By injecting solutions of neural agrin cDNA of increasing transfection efficiencies into denervated SOL muscles, we progressively increased the amounts of neural agrin mRNA and recombinant protein in the muscles. At the lowest concentration, neural agrin induced ectopic clusters of AChRs, which had an average half-life of ≈1 day, like nonaggregated AChRs. At the highest concentration, the average half-life was ≈10 days, as for junctional AChRs at innervated NMJs.

The AChR aggregates induced by neural agrin on denervated unstimulated muscle fibers were numerous and irregularly distributed. During stimulation, most of these aggregates disappeared (the losers) except for a few (the winners) (21). Similar activity-dependent selection of winners and losers occurs during formation of ectopic NMJs by transplanted axons (22). In the present work, winners and losers occurred irrespective of the amount of neural agrin in the muscle. In contrast, AChR half-life at winning sites increased with amount of neural agrin. We attribute the stabilizing effect of neural agrin at winning sites and the elimination of losing sites to different mechanisms. Consistent with this interpretation, full stabilization by neural agrin was activity-independent, whereas elimination of AChRs at losing sites is activity-dependent (21, 22).

Electrical muscle stimulation enhanced AChR stability at ectopic AChR clusters to intermediate values in muscles with low or medium amounts of neural agrin ($t_{1/2}$ = 3.8 or 5.4 days) but had no additional effect in muscles with high amounts of agrin, where agrin alone fully stabilized the receptors ($t_{1/2}$ = ≈10 days). It is of interest to compare the stabilizing effects of stimulation at ectopic clusters and NMJs. At NMJs, denervation destabilizes AChRs in the membrane at the time of denervation (old AChRs, $t_{1/2}$ decreases from ≈10 to 3–7 days), whereas reinnervation restabilizes them. Stimulation has no such restabilizing effect, suggesting that neural agrin or some other factor provided by reinnervating axons is needed (for review see ref. 23). For new AChRs already in the membrane at denervated NMJs when the stimulation starts, the situation is unclear. In our hands, stimulation has no effect on the stability of such receptors (4, 5), nor does reinnervation (24), whereas Caroni *et al.* (6), using similar stimulations, report full stabilization. We have no explanation for this discrepancy. Our present and earlier findings appear consistent in that the stimulation failed to fully stabilize ($t_{1/2}$ = ≈10 days) AChRs already in the membrane of both ectopic AChR clusters and denervated NMJs. For AChRs inserted into the membrane of denervated NMJs after the onset of stimulation, the situation is different. Such receptors become fully stabilized by stimulation (4), suggesting that different mechanisms underlie stabilization of AChRs already in the membrane or on their way to it (see below). Finally, stimulation may affect AChRs at ectopic clusters differently from those at adult NMJs because the ectopic sites are much younger. In addition, NMJs show age-dependent differences because, in the rat, endplates become structurally stable and resistant to AChR dispersal after denervation only by ≈2 weeks after birth (25).

The molecular mechanisms underlying AChR stabilization in muscle are largely unknown. Studies of organ-cultured muscle suggest that stimulation-induced Ca^{2+}-influx and phosphorylation events may mediate some of the stabilizing effects of electrical stimulation (6). Activation of PKA restabilizes AChRs that have been destabilized by denervation (26, 27). Slowly degrading AChRs at normal NMJs, also termed R_s, contain ε-subunits, whereas rapidly degrading extrajunctional AChRs in immature or denervated muscle fibers, also termed R_r, contain γ-subunits. In cultured muscle cells, R_r and R_s behave as distinct molecules that do not interconvert (for review see ref. 23). For example, exogenous dB-cAMP (a cAMP analogue) can stabilize accelerated R_s, whereas ATP cannot. Conversely, ATP can stabilize R_r, but dB-cAMP cannot (28). Consistent with the idea that R_r can be stabilized under certain conditions, we find that ectopic AChRs in nAgrin-low muscles, which are rapidly turning over ($t_{1/2}$ = 0.9 days) and contain predominantly γ-subunits, can be partially stabilized by stimulation ($t_{1/2}$ = 3.8 days). Neuregulin (NRG), another protein produced by motor neurons, stabilizes AChRs on noninnervated myotubes *in vitro* (G.F., unpublished observations). Finally, AChRs at NMJs in mdx mice, which lack dystrophin, have an intermediate half-life (3–5 days) (29), suggesting that cytoskeletal proteins are involved in AChR stabilization. Consistent with this possibility, we have recently found that the organization of dystrophin, β-dystroglycan, syntrophin, and colocalized agrin-induced AChR aggregates depends on electrical muscle stimulation, as well as externally applied purified muscle agrin (30). Electrical activity and/or muscle agrin may therefore contribute to AChR stabilization by affecting the organization of the cytoskeleton. Such mechanisms may also explain the stabilizing effect of stimulation on AChRs that are on their way to the membrane at long-term denervated NMJs where the amount of neural agrin is probably low (ref. 31; see above). Together, these many findings suggest that full AChR stabilization at MNJs is a multifactorial event requiring several signaling pathways.

The full-length isoform of rat agrin used here (14) corresponds to a short NH_2-terminal (SN) isoform that has recently been shown to be expressed in the nervous system of mice and chick together with a long NH_2-terminal (LN) isoform (32, 33). At NMJs in mice, the LN isoform makes up all agrin associated with

the basal lamina (BL), and mutants lacking this form fail to form NMJs (33). However, brain extracts from controls and mutant mice lacking the LN isoform have similar AChR clustering activity (33), consistent with findings that the SN isoform also has synaptic organizing activity. Apparently, in mice, appropriate targeting to motor neurons and BL by LN-agrin is needed (33). An LN-like isoform in rats has not been reported so far. The SN-like isoform used in the present experiments contained a highly conserved ≈1,900-aa sequence common to all identified neural agrins, which included the inserts at sites Y and Z required for synaptic organizing activity (2). This isoform has earlier been shown to induce the formation of a postsynaptic-like apparatus that bear striking resemblance to the postsynaptic apparatus at normal NMJs (11). We therefore interpret the stabilization of AChRs by the SN isoform as an another indication of neural agrin's synaptogenic properties.

In conclusion, we have shown that neural agrin causes dose-dependent increases in metabolic stability of AChRs in the plasma membrane of skeletal muscle fibers. The half-lives of AChRs aggregated by different concentrations of neural agrin were similar to those observed at NMJs under normal or experimental conditions, providing further evidence for neural agrin as master controller of postsynaptic properties at NMJs. However, regulation by other nerve- or muscle-derived factors, such as muscle agrin, may also occur. Modulation of receptor turnover is one means of controlling synaptic strength in neurons (34, 35). The present results suggest that presynaptic factors analogous to neural agrin in muscle may be important in controlling receptor turnover and hence synaptic strength at synapses in the central nervous system.

We are grateful to Dr. J. R. Sanes for antibodies against ε- or γ-subunits, Dr. J. Helm for help with confocal microscopy, Sigrid Schaller for technical assistance, and Dr. M. M. Salpeter for comments on the manuscript. This work was supported by grants from the European Union (EU) Biotechnology Program (BIO4 CT96 0216 and BIO CT96 0433), the Norwegian Research Council (129550/310), and Murst and Telethon (764) (to G.F.). We also thank Professor Letten F. Saugstad's Fund for supporting the confocal microscopy unit.

1. Hall, Z. W. & Sanes, J. R. (1993) *Cell* **72,** 99–121.
2. Sanes, J. R. & Lichtman, J. W. (1999) *Annu. Rev. Neurosci.* **22,** 389–442.
3. Shyng, S. L. & Salpeter, M. M. (1989) *J. Cell Biol.* **108,** 647–651.
4. Fumagalli, G., Balbi, S., Cangiano, A. & Lømo, T. (1990) *Neuron* **4,** 563–569.
5. Andreose, J., Xu, R., Lømo, T., Salpeter, M. M. & Fumagalli, G. (1993) *J. Neurosci.* **13,** 3433–3438.
6. Caroni, P., Rotzler, S., Britt, J. C. & Brenner, H. R. (1993) *J. Neurosci.* **13,** 1315–1325.
7. Salpeter, M. M. & Loring, R. H. (1985) *Prog. Neurobiol.* **25,** 297–325.
8. Salpeter, M. M., Cooper, D. L. & Levitt, G. T. (1986) *J. Cell Biol.* **103,** 1399–1403.
9. McMahan, U. J. (1990) *Cold Spring Harbor Symp. Quant. Biol.* **55,** 407–418.
10. Gautam, M., Noakes, P. G., Moscoso, L., Rupp, F., Scheller, R. H., Merlie, J. P. & Sanes, J. R. (1996) *Cell* **85,** 525–535.
11. Cohen, I., Rimer, M., Lømo, T. & McMahan, U. J. (1997) *Mol. Cell. Neurosci.* **9,** 237–253.
12. Jones, G., Meier, T., Lichtsteiner, M., Witzemann, V., Sakmann, B. & Brenner, H. R. (1997) *Proc. Natl. Acad. Sci. USA* **94,** 2654–2659.
13. Windisch, A., Gundersen, K., Szabolcs, M. J., Gruber, H. & Lømo, T. (1998) *J. Physiol. (London)* **510,** 623–632.
14. Rupp, F., Payan, D. G., Magill, S. C., Cowan, D. M. & Scheller, R. H. (1991) *Neuron* **6,** 811–823.
15. Towbin, H., Staehelin, T. & Gordon, J. (1979) *Proc. Natl. Acad. Sci. USA* **76,** 4350–4354.
16. Turney, S. G., Culican, S. M. & Lichtman, J. W. (1996) *J. Neurosci. Methods* **64,** 199–208.
17. Missias, A. C., Chu, G. C., Klocke, B. J., Sanes, J. R. & Merlie, J. P. (1996) *Dev. Biol.* **84,** 247–254.
18. Gu, Y. & Hall, Z. W. (1988) *Neuron* **1,** 117–125.
19. Frank, E. & Fischbach, G. D. (1979) *J. Cell Biol.* **83,** 143–158.
20. Akaaboune, M., Culican, S. M., Turney, S. G. & Lichtman, J. W. (1999) *Science* **286,** 503–507.
21. Mathiesen, I., Rimer, M., Ashtari, O., Cohen, I., McMahan, U. J. & Lømo, T. (1999) *Mol. Cell. Neurosci.* **13,** 207–217.
22. Skorpen, J., Lafond-Benestad, S. & Lømo, T. (1999) *Mol. Cell. Neurosci.* **13,** 192–206.
23. Salpeter, M. M., Andreose, J., O'Malley, J. P., Xu, R., Fumagalli, G. & Lømo, T. (1993) *Ann. N.Y. Acad. Sci.* **681,** 155–164.
24. Shyng, S. L. & Salpeter, M. M. (1990) *J. Neurosci.* **10,** 3905–3915.
25. Slater, C. R. (1982) *Dev. Biol.* **94,** 23–30.
26. Shyng, S. L., Xu, R. & Salpeter, M. M. (1991) *Neuron* **6,** 469–475.
27. Xu, R. & Salpeter, M. M. (1995) *J. Cell. Physiol.* **165,** 30–39.
28. O'Malley, J. P., Moore, C. T. & Salpeter, M. M. (1997) *J. Cell Biol.* **138,** 159–165.
29. Xu, R. F. & Salpeter, M. M. (1997) *J. Neurosci.* **17,** 8194–8200.
30. Bezakova, G. & Lømo, T. (2001) *J. Cell Biol.*, **153,** 1453–1463.
31. Reist, N. E., Magill, C. & McMahan, U. J. (1987) *J. Cell Biol.* **105,** 2457–2469.
32. Neumann, F. R., Bittcher, G., Annies, M., Schumacher, B., Kroger, S. & Ruegg, M. A. (2001) *Mol. Cell. Neurosci.* **17,** 208–225.
33. Burgess, R. W., Skarnes, W. C. & Sanes, J. R. (2001) *J. Cell Biol.* **151,** 41–52.
34. Mammen, A. L., Huganir, R. L. & O'Brien, R. J. (1997) *J. Neurosci.* **17,** 7351–7358.
35. O'Brien, R. J., Kamboj, S., Ehlers, M. D., Rosen, K. R., Fischbach, G. D. & Huganir, R. L. (1998) *Neuron* **21,** 1067–1078.